

[electromigration into confined spaces]

arXiv:1205.3748v1 [q-bio.QM] 16 May 2012

# The nonlinear electromigration of analytes into confined spaces

BY ZHEN CHEN AND SANDIP GHOSAL

*Northwestern University, Department of Mechanical Engineering  
2145 Sheridan Road, Evanston, IL 60208*

We consider the problem of electromigration of a sample ion (analyte) within a uniform background electrolyte when the confining channel undergoes a sudden contraction. One example of such a situation arises in microfluidics in the electrokinetic injection of the analyte into a micro-capillary from a reservoir of much larger size. Here the sample concentration propagates as a wave driven by the electric field. The dynamics is governed by the Nernst-Planck-Poisson system of equations for ionic transport. A reduced one dimensional nonlinear equation describing the evolution of the sample concentration is derived. We integrate this equation numerically to obtain the evolution of the wave shape and determine how the injected mass depends on the sample concentration in the reservoir. It is shown that due to the nonlinear coupling of the ionic concentrations and the electric field, the concentration of the injected sample could be substantially less than the concentration of the sample in the reservoir.

**Keywords:** electromigration dispersion, electrokinetic injection, nonlinear waves

## 1. Introduction

In microfluidic systems, electrokinetic injection is often employed in order to insert the sample from a reservoir into a microfluidic channel (Landers, 1996; Camilleri, 1998). A simplified problem depicting the electrokinetic injection process is shown in Figure 1. The reservoir initially contains the sample dissolved in a background electrolyte of positive and negative ions. The channel contains only the background electrolyte. At time  $t = 0$ , a voltage,  $V$  is applied to an electrode in the reservoir located far from the inlet, while the channel outlet (assumed infinitely far away) is electrically grounded. We would like to describe how the concentration of the sample evolves with time as the sample moves into the micro-channel. For simplicity, we will assume that the capillary walls are uncharged so that there is no electroosmotic flow.

When the concentration of sample in the reservoir is low, the dynamics is linear and is described by an advection diffusion equation with constant advection speed. At high concentrations, the evolution is nonlinear due to the phenomenon of electromigration dispersion. The physical mechanism of electromigration dispersion may be explained (Ghosal & Chen, 2010a) in the following way: when the concentration of sample ions is significant in comparison to that of the background electrolyte, the electrical conductivity of the solution is locally altered. However, charge conservation and local electro neutrality requires the electric current to be the same

at all points along the axis of the capillary. Therefore, by Ohm's law, (ignoring, for the moment, the diffusive contributions to the current), the electric field must change axially, since, the product of the conductivity and electric field must remain constant. This varying electric field alters the effective migration speed of the sample ions, which in turn, alters its concentration distribution. The transport problem for sample ions then becomes nonlinear and shock like structures similar to those familiar from breaking water waves (Whitham, 1974) can arise.

The problem has a certain similarity with the classical "dam break problem" in hydrodynamics where a large stationary volume of water held back by a wall is suddenly released by partial or complete removal of the restraining wall (Whitham, 1955; Stoker, 1948; Ritter, 1892). However, in the present problem, the driving mechanism is the variation of the electric field along the channel instead of hydrostatic pressure variations due to changes in wave height.

In the next section we present the mathematical formulation for a minimal problem consisting of three ionic species - the analyte, a co-ion and a counter-ion, where the diffusivities of the three species are equal, the charge of the analyte is constant, and, the background electrolyte is fully dissociated. We will see that even in this highly idealized limit, the nonlinearities inherent in the system lead to surprising behavior. The idealizations permit reduction of the problem to the solution of a single partial differential equation in one dimension. In section 3, this equation is integrated numerically, and observations are presented for the behavior of the sample ion concentration as it moves into the micro-channel. We find that at high concentrations, the concentration of sample ions that enter the micro-channel is significantly lower than that in the reservoir. In fact, as the concentration of sample ions in the reservoir is increased, the concentration within the injected plug in the channel does not increase indefinitely; but, approaches a limiting value determined by the valence of the analyte ion and background electrolytes. In section 4, we identify the reason for this behavior and use simple arguments based on conservation laws to deduce the limiting value of the sample concentration in the channel. This is compared to results from the numerical simulations and good agreement is found. Our findings are summarized in section 5 and its implications in a broader context as well as its limitations are discussed.

## 2. Problem Formulation

We consider a three ion system consisting of sample ions, co-ions and counterions all of equal diffusivity ( $D$ ). It follows, from the Einstein relation, that the mobility ( $u$ ) of the three ionic species are also the same. However, the three species have different valences:  $z_p, z_n, z$  and therefore different electrophoretic mobilities:  $\mu_p = z_p eu, \mu_n = z_n eu, \mu = zeu$ ,  $e$  being the proton charge. In this paper, the suffix  $p$  will generally indicate the positive ion (cation),  $n$  will indicate the negative ion (anion) and the absence of a suffix will indicate the sample ion (analyte). Thus,  $z_p$  is positive,  $z_n$  is negative and  $z$  could be of either sign. The discussion in the rest of this section follows closely the earlier work of Ghosal & Chen (2010a).

We consider the simplest situation where the ions migrate from a semi-infinite reservoir to a uniform channel with no wall charge. Then the problem is entirely one dimensional, and, the coupled equations describing the concentrations of the

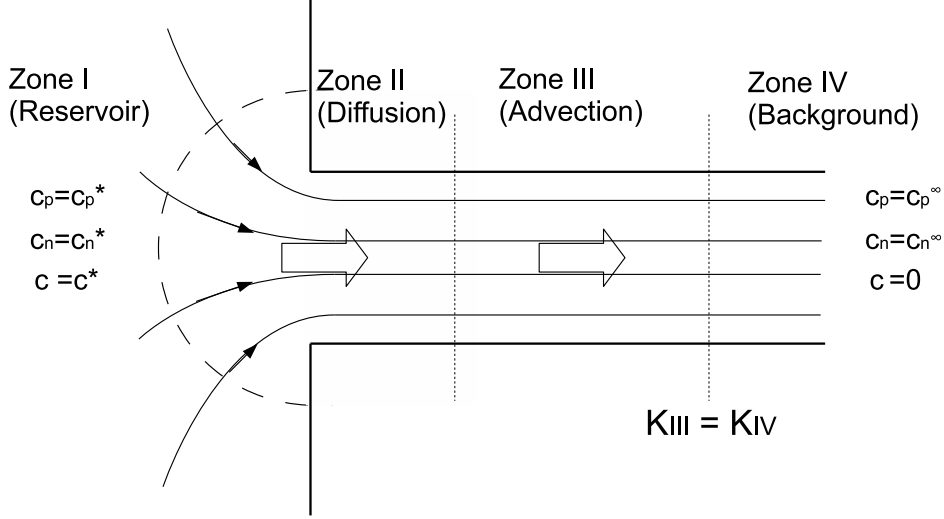


Figure 1. Schematic diagram illustrating the electrokinetic injection of a sample (concentration  $c^*$  in the reservoir) into a micro-channel

three ion species are

$$\frac{\partial c_p}{\partial t} + \frac{\partial}{\partial x} (z_p e u E c_p) = D \frac{\partial^2 c_p}{\partial x^2}, \quad (2.1)$$

$$\frac{\partial c_n}{\partial t} + \frac{\partial}{\partial x} (z_n e u E c_n) = D \frac{\partial^2 c_n}{\partial x^2}, \quad (2.2)$$

$$\frac{\partial c}{\partial t} + \frac{\partial}{\partial x} (z e u E c) = D \frac{\partial^2 c}{\partial x^2}, \quad (2.3)$$

where  $E$  is the local electric field,  $x$  is the distance along the capillary and  $t$  is time. We will assume that the  $x$ -axis points in the direction of front motion from the reservoir into the capillary. Since characteristic spatial scales are always much larger than the Debye length, local electro-neutrality holds (Ghosal & Chen, 2010). Thus,

$$z_p c_p + z_n c_n + z c = 0. \quad (2.4)$$

If we multiply equations (2.1)-(2.3) by the respective ionic charges, sum them, and use equation (2.4), we get an equation that describes the constancy of electric current

$$\frac{\partial}{\partial x} [e^2 u (z_p^2 c_p + z_n^2 c_n + z^2 c) E] = 0. \quad (2.5)$$

Note, that, the net contribution from the diffusive fluxes vanish exactly on account of the assumption of equal diffusivity of ions and local electro-neutrality. Equation (2.5) may then be integrated to yield

$$(z_p^2 c_p + z_n^2 c_n + z^2 c) E = (z_p^2 c_p^\infty + z_n^2 c_n^\infty) E_\infty, \quad (2.6)$$

where  $E_\infty$  is the electric field in the capillary very far away from the inlet, and,  $c_n^\infty, c_p^\infty$  are respectively the corresponding negative and positive ion concentrations

in the background electrolyte. Clearly,  $c_p^\infty$  and  $c_n^\infty$  are not independent but are related by the electro-neutrality condition

$$z_p c_p^\infty + z_n c_n^\infty = 0. \quad (2.7)$$

If we now introduce the Kohlrausch function (Kohlrausch, 1897)

$$K(x, t) = (c_p + c_n + c)/u, \quad (2.8)$$

then it follows from equations (2.1)-(2.3) and (2.4) that  $K$  satisfies the diffusion equation

$$\frac{\partial K}{\partial t} = D \frac{\partial^2 K}{\partial x^2}. \quad (2.9)$$

The three algebraic relations: (2.4), (2.6) and (2.8), may be used to express all four dependent variables in the problem:  $c_p, c_n, c$  and  $E$  in terms of any one of them and the function  $K(x, t)$ . We choose to express all the variables in terms of  $c$  and  $K$ . These relations take a particularly simple form if we use the normalized concentration

$$\phi = \frac{c}{c_n^\infty} \quad (2.10)$$

and

$$\theta(x, t) = \frac{uz_p}{z_p - z_n} \frac{K(x, t)}{c_n^\infty} \quad (2.11)$$

In terms of these variables, we then have

$$E = \frac{E_\infty}{\theta - \alpha\phi}, \quad (2.12)$$

$$\phi_p = \frac{c_p}{c_n^\infty} = -\frac{z - z_n}{z_p - z_n} \phi - \frac{z_n}{z_p} \theta, \quad (2.13)$$

$$\phi_n = \frac{c_n}{c_n^\infty} = \frac{z - z_p}{z_p - z_n} \phi + \theta, \quad (2.14)$$

so that, equation (2.3) gives the following evolution equation for  $\phi$ :

$$\frac{\partial \phi}{\partial t} + \frac{\partial}{\partial x} \left( \frac{v\phi}{\theta - \alpha\phi} \right) = D \frac{\partial^2 \phi}{\partial x^2}, \quad (2.15)$$

where  $v = zeuE_\infty$  is the velocity of an isolated sample ion in the constant electric field  $E = E_\infty$ , and, following the notation of Ghosal & Chen (2010a),  $\alpha = [(z - z_n)(z - z_p)/z_n(z_p - z_n)]$ , is the ‘‘velocity-slope parameter’’.

Since  $\theta$  is proportional to  $K$ , it is also a passive scalar. The initial and boundary conditions on  $\theta$  in the domain  $0 \leq x < \infty$  are

$$\theta(x, 0) = 1 \quad \text{if } x > 0, \quad (2.16)$$

$$\theta(0, t) = \theta^*, \quad (2.17)$$

$$\theta(\infty, t) = 1, \quad (2.18)$$

where  $\theta^*$  is the value of  $\theta$  in the reservoir. The reservoir is considered to be ‘‘well mixed’’ so that all ionic concentrations remain constant within it. An exact solution for  $\theta$  may then be found using Fourier’s method,

$$\theta = \theta^* + (1 - \theta^*) \operatorname{erf} \left( \frac{x}{\sqrt{4Dt}} \right), \quad (2.19)$$

where

$$\operatorname{erf}(x) = \frac{2}{\sqrt{\pi}} \int_0^x e^{-y^2} dy \quad (2.20)$$

is the error function. Since the concentration of sample in the reservoir is being held constant at some value  $\phi = \phi^*$ , we have

$$\theta^* = \frac{c_n^*}{c_n^\infty} + \frac{z_p - z}{z_p - z_n} \phi^*. \quad (2.21)$$

The superscript  $*$  indicates the value of the corresponding variable in the reservoir. Thus,  $c_n^*$  is the concentration of negative ions in the reservoir.

Equation (2.15), on the other hand, does not readily admit an analytical solution, since, unlike the equation for  $\theta$ , it cannot be reduced to an ordinary differential equation by means of the similarity variable  $\eta = x/\sqrt{4Dt}$ . We will therefore obtain the time evolution of the normalized sample concentration  $\phi(x, t)$  by substituting equation (2.19) in equation (2.15) and integrating the resulting one dimensional partial differential equation numerically. Before we present this solution in the next section, it is useful to note that at large distances from the reservoir, or more precisely, if  $x \gg \sqrt{4Dt}$ , equation (2.19) implies that  $\theta \sim 1$ , so that equation (2.15) reduces to

$$\frac{\partial \phi}{\partial t} + \frac{\partial}{\partial x} \left( \frac{v\phi}{1 - \alpha\phi} \right) = D \frac{\partial^2 \phi}{\partial x^2} \quad (2.22)$$

which was studied earlier by Ghosal & Chen (2010a).

### 3. Numerical Simulations

We will find it convenient to express our results in terms of a characteristic length,  $w$  (the channel width), which gives a characteristic time  $w/v$ . Then clearly, the only parameters in the problem are  $Pe = vw/D$ , which may be regarded as a ‘‘Péclet number’’ based on the electromigration speed,  $v$ , or a ‘‘field strength parameter’’; the two valence ratios  $z_n/z$ ,  $z_p/z$ ; and, the parameter  $\theta^*$  characterizing the ionic composition of the mixture in the reservoir. For definiteness, we will assume that the sample is a cation ( $z > 0$ ), and that

$$c_p^* = c_p^\infty \quad (3.1)$$

This will be true, for example, if the electrolyte in the reservoir is prepared by adding the sample in solid form (so there is no dilution) to a stock solution of the background electrolyte that fills the micro-channel (since the sample contributes only counter-ions, the co-ion concentration is not altered). Using the electro-neutrality conditions,

$$\theta^* = 1 - \frac{z_p(z - z_n)}{z_n(z_p - z_n)} \phi^*. \quad (3.2)$$

The initial and boundary conditions for  $\phi$  are

$$\phi(x, 0) = 0, \quad \text{if } x > 0 \quad (3.3)$$

$$\phi(0, t) = \phi^*, \quad (3.4)$$

$$\phi(\infty, t) = 0. \quad (3.5)$$

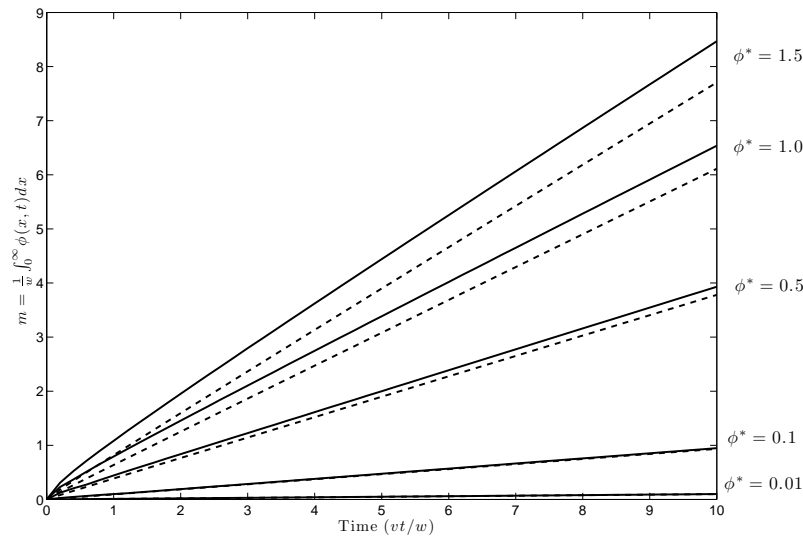


Figure 2. The increase of sample ions in the micro-channel as a function of dimensionless time at different dimensionless reservoir concentrations,  $\phi^*$ . The solid line corresponds to  $Pe = 10$  and the dashed line corresponds to  $Pe = 200$ .

We keep the valence ratios fixed at  $z_p/z = 2$ ,  $z_n/z = -1$ .

Since we have reduced our problem to a one dimensional one, the numerical integration is quite straightforward. We used a finite volume method to discretize equation (2.15) in space using an adaptive grid refinement algorithm that is enabled by applying the Matlab library “MatMOL” (Vande Wouwer *et al.*, 2004). The spatially discretized system of equations is then integrated in time using the Matlab solver “ode45” (Shampine & Reichelt, 1997) which is based on an explicit Runge-Kutta (4,5) formula.

Figure 2 shows the amount of sample that has moved into the reservoir at time  $t$ , defined as

$$m(t) = \frac{1}{w} \int_0^\infty \phi(x, t) dx. \quad (3.6)$$

Simulations are shown for  $Pe = 10$  and  $200$ . At long times, or more precisely, if  $vt/w \gg Pe^{-1}$ , the expected asymptotic form for  $m(t)$  is

$$m(t) \sim (v\phi^*/w)t. \quad (3.7)$$

Figure 2 shows that indeed, at large times,  $m(t) \propto t$ . We determined the slope of the  $m(t)$  curve at large times and plotted the dimensionless quantity  $w\dot{m}/v$  as a function of  $\phi^*$  in Figure 3. It is seen that  $w\dot{m}/v \sim \phi^*$  as long as  $\phi^* \ll 1$  but as the concentration of sample in the reservoir is increased, the injection rate does not increase indefinitely but tends to saturate to a limiting value, that is,  $w\dot{m}/v \sim \phi_m^* < \phi^*$ .

The reason for this saturation of the injection rate may be understood by examining the concentration profiles  $\phi(x, t)$  shown in Figure 4. It is seen, that as the

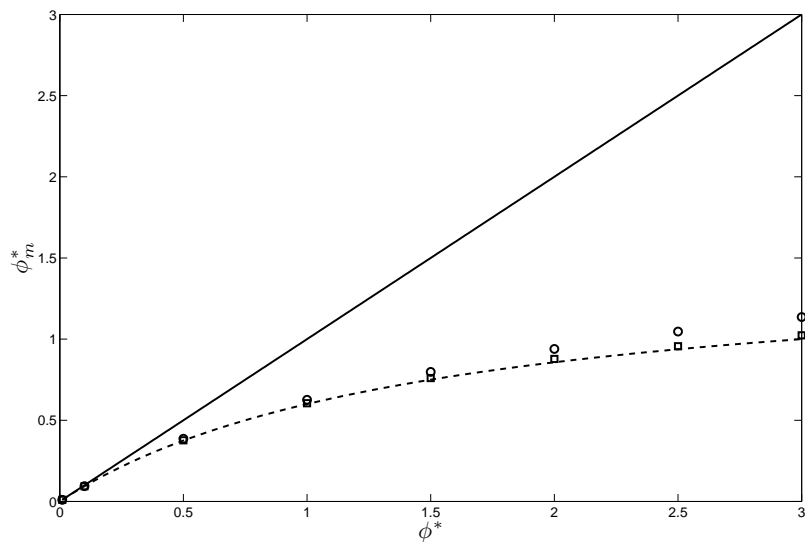


Figure 3. The normalized concentration of analyte in the micro-channel ( $\phi_m^*$ ) as a function of the corresponding quantity in the reservoir ( $\phi^*$ ). The solid line indicates the result expected from linear theory, the dashed line is the result predicted by the nonlinear theory, equation (4.7). The symbols (circle:  $Pe=10$ , square:  $Pe=200$ ) are obtained by numerical integration of equation (2.15).

sample moves into the capillary, the concentration in the capillary is approximately equal to the the concentration in the reservoir as long as this concentration remains small (upper panel,  $\phi^* = 0.01$ ). However, if the concentration in the reservoir is large (lower panel,  $\phi^* = 1.0$ ) the concentration in the channel approaches a limiting value  $\phi_m^*$  independent of the reservoir concentration.

In Figure 5, we have reproduced the concentration distribution  $\phi(x, t)$  that appears in the lower panel of Figure 4, together with the concentrations of the other ionic species  $\phi_p(x, t)$  and  $\phi_n(x, t)$ , the local electric field  $E(x, t)$ , and, the local electrical conductivity due to ions,  $\sigma(x, t)$ . These quantities are obtained from equations (2.12), (2.13) and (2.14). The mechanism for the reduction of the concentration from  $\phi = \phi^*$  in the reservoir to  $\phi = \phi_m^* < \phi^*$  in the capillary may be understood from these graphs. At large values of the sample concentrations in the reservoir, there is a sharp rise in the solution conductivity in the immediate vicinity of the inlet resulting in a drop in the electric field. The flux of sample into the micro-channel is then determined by a combination of this greatly reduced electromigrational flux and the diffusive flux and this is less than the expected flux indicated by equation (3.7), which should hold in the linear regime.

#### 4. Analysis

An approximate theoretical determination of the critical concentration  $\phi_m^*$  may be provided using the conservation equations. The method of doing this is in fact entirely analogous to that of the ‘‘Moving Boundary Equations’’ (MBE) (Dole, 1945)

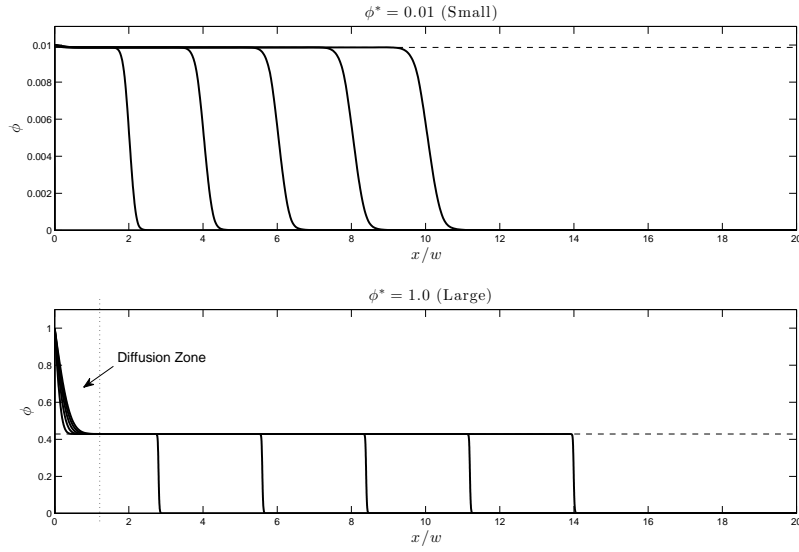


Figure 4. Concentration profiles in the micro-capillary at successive times:  $vt/w = 2, 4, 6, 8, 10$ . If the reservoir concentration is large (lower panel), a concentration jump develops at the entrance of the capillary, with a narrow diffusion zone connecting the values in the reservoir with the much smaller value of the concentration within the capillary. The concentration jump is insignificant if the reservoir concentration is small (upper panel). The dashed line is  $\phi_m^*$  evaluated using equation (4.8). Here  $Pe=200$ .

for describing advancing fronts (e.g. in isotachopheresis). The conceptual framework is illustrated in Figure 1. The domain is decomposed into four parts: (I) the “Reservoir Zone” within the well mixed body of the reservoir where all concentrations are constant (II) the “Diffusion Zone” which is the initial part of the micro-channel of length of order  $\sqrt{2Dt}$  – here the ionic diffusive flux and the electromigrational flux driven by the electric field are comparable, (III) the “Advection Zone” where diffusive fluxes are negligible (because concentration gradients are small) and ionic fluxes are primarily due to electromigration, and, (IV) the “Background Zone” far downstream where the sample ions have not yet penetrated.

The boundary between the Zones (I) and (II) is stationary (and located at the channel inlet) whereas the boundaries between the other zones propagate to the right. The arrows in Figure 1 indicate fluxes of ions across the stationary zone boundary. Equality of the fluxes for each species across the zone boundary require:

$$\pi r \phi^* E^{(I)}(r) = w E^{(III)} \phi_m^* \quad (4.1)$$

$$\pi r \phi_n^* E^{(I)}(r) = w E^{(III)} \phi_n^{(III)} \quad (4.2)$$

where  $E^{(I)}(r)$  represents the electric field in the reservoir at a radial distance  $r$  from the inlet. The superscript (I), (II), (III) or (IV) indicate the zone in which the corresponding variable is evaluated. Clearly  $\phi^{(I)} = \phi^*$ ,  $\phi_n^{(I)} = \phi_n^*$  and  $\phi^{(III)} = \phi_m^*$ . Therefore, taking the ratio,

$$\phi_n^* = (\phi_n^{(III)} / \phi_m^*) \phi^* \quad (4.3)$$

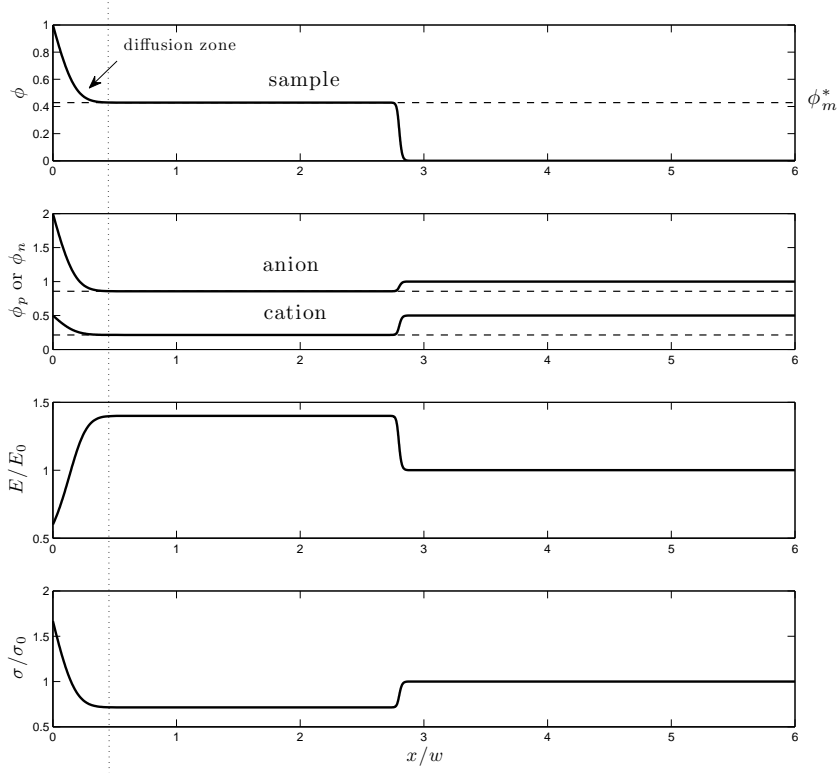


Figure 5. Same as in Figure 4 except that profiles of all dependent variables are shown but at a fixed time instant,  $vt/w = 2$ . The dashed lines are the concentrations in the capillary calculated using equation (4.7). The bottom panel shows the electric conductivity ( $\sigma$ ) normalized by its downstream value ( $\sigma_0$ ).

The Kohlrausch function, or, equivalently,  $\theta(x, t)$ , propagates only by diffusion. Therefore,  $\theta(x, t)$  differs from unity only in Zones (I) and (II). Thus,

$$\phi_n^{(III)} + \phi_p^{(III)} + \phi_m^* = 1 \quad (4.4)$$

The electro-neutrality condition (valid in all zones) for Zone (III) is:

$$z_p \phi_p^{(III)} + z_n \phi_n^{(III)} + z \phi_m^* = 0. \quad (4.5)$$

By combining equations (4.3) and (4.4) and using the electro-neutrality condition, equation (4.5), we get an equation for determining  $\phi_m^*$

$$(1 - z/z_p) \phi_m^* + r(1 - z_n/z_p) \phi_m^* = 1 - z_n/z_p, \quad (4.6)$$

where the ratio  $\phi_n^*/\phi^* = r$  is a constant determined by the ionic composition of the electrolyte in the reservoir. Solving the above linear equation for  $\phi_m^*$  we have

$$\phi_m^* = [r + (z_p - z)/(z_p - z_n)]^{-1}. \quad (4.7)$$

In our numerical experiment we assume that the sample is a cation, and that the co-ion concentration in the reservoir is the same as in the channel, so that  $\phi_p^* = \phi_p^\infty = -z_n/z_p$ . The electro-neutrality condition then implies that  $\phi_n^* = 1 - (z/z_n)\phi^*$ , so that equation (4.7) becomes

$$\phi_m^* = \frac{\phi^*}{1 + \xi\phi^*} \quad (4.8)$$

where

$$\xi = -\frac{z_p(z - z_n)}{z_n(z_p - z_n)} \quad (4.9)$$

is a positive number. An expression for  $\theta^*$  in terms of the sample ion concentration,  $\phi^*$ , may also be derived by simple algebra:

$$\theta^* = 1 - \frac{z_p(z - z_n)}{z_n(z_p - z_n)}\phi^*. \quad (4.10)$$

In Figure 3, we used equation (4.8) to plot  $\phi_m^*$  as a function of  $\phi^*$ . This curve is seen to describe very well the nonlinear saturation of the injected mass with increasing sample concentration in the reservoir.

The denominator in equation (2.15) vanishes if  $\phi = \theta/\alpha$ . Far from the inlet, the singularity is approached as  $\phi \rightarrow 1/\alpha$  (if  $\alpha > 0$ ), since,  $\theta \sim 1$ . It was shown earlier (Ghosal & Chen, 2010a) that the requirement of positivity of all ionic concentrations imposes a condition of self-consistency,  $\phi(x, t) < \phi_c$  where

$$\phi_c = \begin{cases} (z_p - z_n)/(z_p - z) & \text{if } z > 0 \\ -[z_n(z_p - z_n)]/[z_p(z - z_n)] & \text{if } z < 0. \end{cases} \quad (4.11)$$

Since,  $\phi_c < 1/\alpha$ , if  $\alpha > 0$  (see Appendix), the singularity is never reached if initially  $\phi$  is less than  $\phi_c$  everywhere in the channel. This, however, leaves open the possibility that the initial condition  $\phi(0, t)$  might be such, that,  $\phi$  exceeds  $\phi_c$  in some parts of the domain. We have now shown that if electrokinetic injection is used to insert the sample into the capillary, the shock at the inlet ensures that the injected sample concentration does not exceed  $\phi_m^* < \phi_c$  (see Appendix), no matter how high the sample concentration in the reservoir may be. In capillary zone electrophoresis, one chooses the peak shape after electrokinetic sample injection as the ‘‘initial condition’’. Then, the only initial conditions possible are the ‘‘realizable’’ kind, where,  $\phi(x, 0) < \phi_c$ .

The speed of propagation of the analyte front in Figure 4 may be readily calculated when the front is far from the inlet. To do this, we note that since  $Pe = 200 \gg 1$  and  $\theta \rightarrow 1$ , equation (2.22) may be written as

$$\frac{\partial\phi}{\partial t} + \frac{\partial Q}{\partial x} = 0 \quad (4.12)$$

where

$$Q(\phi) = \frac{v\phi}{1 - \alpha\phi}. \quad (4.13)$$

Then, the shock propagation speed is given by (Whitham, 1974) the Rankine-Hugoniot jump condition

$$V_s = \frac{Q(\phi_2) - Q(\phi_1)}{\phi_2 - \phi_1} \quad (4.14)$$

where the subscripts 2 and 1 refer to conditions just behind the shock and just ahead of the shock respectively. Putting  $\phi_1 = 0$  and  $\phi_2 = \phi_m^*$ , we find, for the conditions shown in the lower panel of Figure 4,  $\phi_m^* = 3/7 \approx 0.43$ , so that,  $V_s = 1.405 v$ . The shock speed determined from direct measurement of the front displacement in Figure 4 is  $1.4 v$ , in close agreement with the theoretical prediction. In the upper panel,  $\phi^* = 0.01$ , so that  $\phi_m^* \approx \phi^*$ . In this case, both the theoretical and the measured values give  $V_s \approx v$ .

## 5. Conclusions

The problem of electromigration of a sample ion from a large reservoir into a confined channel in the presence of a fully dissociated background electrolyte was studied in the idealized situation where all ionic species have the same diffusivity. If the sample ion concentration is small compared to that of the background electrolyte, the behavior of the system is exactly as one might expect. When the electric field is switched on, a sample plug with concentration equal to that in the reservoir, is drawn into the microchannel. However, if the sample ion concentration is comparable or large compared to the background electrolyte, the behavior of the system is dominated by the intrinsic nonlinearity of the electro-diffusional problem, and the outcome is quite counter-intuitive. Once again, the sample is drawn into the microchannel as a plug of increasing length, but the concentration of sample ions in the plug is less than in the reservoir. In fact, as the reservoir concentration is progressively increased, the concentration of sample ions in the capillary approaches a limit that depends on the valences of the three ionic species but is independent of the reservoir concentration.

In an earlier paper (Ghosal & Chen, 2010a), the authors presented a theory of electromigration of a sample in an infinitely long micro-channel when only three ions of equal diffusivity are present. There, it was shown, that, the requirement that none of the three ionic concentrations could ever be negative, put a limit to the validity of the theory. It was therefore required that the initial condition be such, that, the dimensionless sample concentration not exceed a certain (positive) critical concentration,  $\phi_c$ . Here we have shown that initial conditions that do not satisfy this requirement cannot arise if the analyte is introduced into the micro-capillary by electrokinetic injection. In fact, the diffusional boundary layer at the channel entrance ensures that the concentration of analyte drawn into the micro-capillary is always less than  $\phi_c$ . Thus, the critical concentration can never be exceeded if the sample is introduced by electrokinetic injection, and consequently, the singularity at  $\phi = 1/\alpha$  (if  $\alpha > 0$ ), inherent in equation (2.22) is never reached.

One may question whether the strongly nonlinear regime considered here is of relevance to actual laboratory practice. The answer depends on the numerical value of the critical concentrations,  $\phi_m^*$  and  $\phi_c$ . If the sample and carrier ions have similar valences, then these critical concentrations are all of order unity. Thus, to approach these critical values, the sample ions in the injected plug will need to be present at concentrations approaching that of the carrier electrolyte. Such high concentrations are normally not employed in laboratory practice with capillary electrophoresis. However, if the sample is a macro-ion the critical values may actually be quite small. For example, at pH 2.0 Bovine serum albumin has a valence,  $z \sim 55$  (Ford & Winzor, 1982). Then, in a univalent carrier electrolyte we

have  $\phi_c \sim 0.04$ , so that the strongly nonlinear regime studied here may be easily reached.

The shock like transition in concentration at the entrance of the micro-channel observed here is reminiscent of “de-salination shocks” that propagate outward from micro-channel/nano-channel junctions (Mani, Zangle & Santiago, 2009; Zangle, Mani & Santiago, 2009) or from the surface of a perm-selective membrane embedded in a microfluidic channel. The mechanism of these shocks is related to the nonlinear coupling between the ion depletion zone (due to concentration polarization) near the membrane with the electric Debye layers at the walls of the micro-channel. The problem considered here is much simpler; Debye layers or concentration polarization are not involved. Nevertheless, it is another example of shock-like behavior that may be traced to the nonlinear nature of the underlying Nernst-Planck-Poisson system of equations for ionic transport. As in the case of de-salination shocks, the effect described here would also be relevant for solutes electromigrating into porous media (Mani & Bazant, 2011) or electromigration of analytes through variable geometry channels, such as pores in membranes, where lubrication theory (Ghosal, 2002) can be used to generalize the analysis presented here. Finally, if the channel walls are charged, electroosmotic flow would arise so that the transport problem becomes intrinsically two or three dimensional. In such cases, homogenization can be used to achieve a reduced description, as shown by Ghosal & Chen (2012) for electromigration in an infinitely long uniform channel.

*Acknowledgement:* Support from the National Institute of Health (NIH) under grant R01EB007596 is gratefully acknowledged.

## References

- Camilleri, P. (ed.) 1998 *Capillary electrophoresis, theory & practice*. Boca Raton, U.S.A.: CRC Press.
- Dole, V. P. 1945 A theory of moving boundary systems formed by strong electrolytes1. *Journal of the American Chemical Society*, **67**(7), 1119–1126. (doi:10.1021/ja01223a025)
- Ford, C. L. & Winzor, D. J. 1982 Measurement of the net charge (valence) of a protein. *Biochimica et Biophysica Acta (BBA) - Protein Structure and Molecular Enzymology*, **703**(1), 109–112. (doi:16/0167-4838(82)90017-6)
- GHOSAL, S. 2002 Lubrication theory for electroosmotic flow in a microfluidic channel of slowly varying cross-section and wall charge. *J. Fluid Mech.* **459**, 103–128.
- Ghosal, S. & Chen, Z. 2010 A nonlinear equation for ionic diffusion in a strong binary electrolyte. *Proc. Royal Soc. Lond. A*, **466**, 2145–2154.
- Ghosal, S. & Chen, Z. 2010a Nonlinear waves in capillary electrophoresis. *Bulletin of Mathematical Biology*, **72**(8), 2047–2066.
- GHOSAL, S. & CHEN, Z. 2012 Electromigration dispersion in a capillary in the presence of electro-osmotic flow. *J. Fluid Mech.* **697**, 436–454.

- Kohlrausch, F. 1897 Ueber concentrations-verschiebungen durch electrolyse im inneren von lösungen und lösungsgemischen. *Ann. Phys.*, **62**, 209–239.
- Landers, J. (ed.) 1996 *Introduction to capillary electrophoresis*. Boca Raton, U.S.A.: CRC Press.
- Mani, A., Zangle, T.A. & Santiago, J.G. 2009 On the Propagation of Concentration Polarization from Microchannel–Nanochannel Interfaces Part I: Analytical Model and Characteristic Analysis *Langmuir*, **25**(6), 3898–3908.
- Mani, A. & Bazant, M.Z. 2011 Deionization shocks in microstructures. *Phys. Rev. E*, **84**(6), 061504.
- Ritter, A. 1892 Die fortpflanzung der wasserwellen. *Ver Deutsch ingenieur zeitschr*, **36**(33), 947–954.
- Shampine, L. F. & Reichelt, M. W. 1997 The MATLAB ODE suite. *SIAM Journal on Scientific Computing*, **18**(1), 1.
- Stoker, J. 1948 The formation of breakers and bores. *Commun. Appl. Math.*, **1**, 1–87.
- Vande Wouwer, A., Saucez, P. & Schiesser, W. E. 2004 Simulation of distributed parameter systems using a Matlab-Based method of lines toolbox: chemical engineering applications. *Industrial & Engineering Chemistry Research*, **43**(14), 3469–3477. (doi:10.1021/ie0302894)
- Whitham, G. 1974 *Linear and nonlinear waves*. New York, U.S.A.: Wiley-Interscience.
- Whitham, G. B. 1955 The effects of hydraulic resistance in the Dam-Break problem. *Proceedings of the Royal Society of London. Series A, Mathematical and Physical Sciences*, **227**(1170), 399–407.
- Zangle, T.A., Mani, A. & Santiago, J.G. 2009 On the Propagation of Concentration Polarization from Microchannel–Nanochannel Interfaces Part II: Numerical and Experimental Study *Langmuir*, **25**(6), 3909–3916.

### Appendix: Proof of the inequality $\phi_m^* < \phi_c < 1/\alpha$

If  $\alpha > 0$ ,  $z_p > z > z_n$ . Then

$$\alpha\phi_c = \begin{cases} \frac{z_p - z_n}{z_p - z} \frac{(z - z_n)(z - z_p)}{z_n(z_p - z_n)} = \frac{-z_n + z}{-z_n} < 1 & \text{if } z < 0 \\ -\frac{z_n}{z_p} \cdot \frac{z_p - z_n}{z - z_n} \frac{(z - z_n)(z - z_p)}{z_n(z_p - z_n)} = \frac{z_p - z}{z_p} < 1 & \text{if } z > 0 \end{cases} \quad (\text{A-1})$$

thus,  $\phi_c < 1/\alpha$  if  $\alpha > 0$ .

To prove the first part of the inequality,  $\phi_m^* < \phi_c$ , we first show that  $r > -z/z_n$ . This is clearly true if  $z < 0$ . To show this when  $z > 0$ , first we use the electro-neutrality condition to express  $\phi_p^*$  in terms of the other variables:

$$\phi_p^* = -\frac{z}{z_p}\phi^* - \frac{z_n}{z_p}\phi_n^* = \frac{\phi^*}{z_p}(-z - rz_n). \quad (\text{A-2})$$

Now we must have  $\phi_p^* > 0$ . This is always true if  $z < 0$ , but if  $z > 0$ , we require that  $r > -z/z_n$ .

We will now show that  $\phi_m^* < \phi_c$  by considering the two cases  $z > 0$  and  $z < 0$  separately. First suppose that  $z < 0$ . Then

$$\phi_m^* = \frac{1}{r + (z_p - z)/(z_p - z_n)} < \frac{1}{(z_p - z)/(z_p - z_n)} = \frac{z_p - z_n}{z_p - z} = \phi_c \quad (\text{A-3})$$

Now suppose that  $z > 0$ . Then

$$\phi_m^* = \frac{1}{r + (z_p - z)/(z_p - z_n)} \quad (\text{A-4})$$

$$< \frac{1}{-(z/z_n) + (z_p - z)/(z_p - z_n)} = -\frac{z_n}{z_p} \frac{z_p - z_n}{z - z_n} = \phi_c \quad (\text{A-5})$$

Thus, in all cases,  $\phi_m^* < \phi_c$  which completes the proof.